

# Cysteine-scanning Analysis of Putative Helix XII in the YgfO Xanthine Permease

## ILE-432 AND ASN-430 ARE IMPORTANT<sup>3</sup>

Received for publication, January 10, 2008 Published, JBC Papers in Press, March 21, 2008, DOI 10.1074/jbc.M800261200

Konstantinos Papakostas, Ekaterini Georgopoulou, and Stathis Frillingos<sup>1</sup>

From the Laboratory of Biological Chemistry, University of Ioannina Medical School, 45110 Ioannina, Greece

Transmembrane helix XII of UapA, the major fungal homolog of the nucleobase-ascorbate transporter (NAT/NCS2) family, has been proposed to contain an aromatic residue acting as a purine-selectivity filter, distinct from the binding site. To analyze the role of helix XII more systematically, we employed Cys-scanning mutagenesis of the *Escherichia coli* xanthine-specific homolog YgfO. Using a functional mutant devoid of Cys residues (C-less), each amino acid residue in sequence <sup>419</sup>ILPASIYVLVENPICAGGLTAILLNILPGGY<sup>450</sup> (the putative helix XII is underlined) was replaced individually with Cys. Of the 32 single-Cys mutants, 25 accumulate xanthine to 80–130% of the steady state observed with C-less YgfO, six (P421C, S423C, I424C, Y425C, L427C, G436C) accumulate to low levels (15–40%), and I432C is inactive. Immunoblot analysis shows that P421C and I432C display low expression in the membrane. Extensive mutagenesis reveals that replacement of Ile-432 with equally or more bulky side chains abolishes active transport without affecting expression, whereas replacement with smaller side chains allows activity but impairs affinity for the analogues 1-methyl and 6-thioxanthine. Only three of the single-Cys mutants of helix XII (V426C, N430C, and N443C) are sensitive to inactivation by *N*-ethylmaleimide. N430C is highly sensitive, with an IC<sub>50</sub> of 10 μM, and is completely protected against inactivation in the presence of 2-thioxanthine, a high affinity substrate analogue. Other xanthine analogues are poorly bound by N430C, whereas replacement of Asn-430 with Thr inactivates the permease. The findings suggest that Ile-432 and Asn-430 of helix XII are crucial for purine uptake and affinity, and Asn-430 is probably at the vicinity of the binding site.

The nucleobase-ascorbate transporter (NAT)<sup>2</sup> or nucleobase-cation symporter-2 (NCS2) family is an evolutionarily

ubiquitous family of purine, pyrimidine, and L-ascorbate transporters, with members specific for the cellular uptake of uracil, xanthine, or uric acid (microbial and plant genomes) or vitamin C (mammalian genomes) (1–3). Despite their importance as molecular gateways for the recognition and uptake of several frontline purine-related drugs, NAT/NCS2 members have not been studied systematically at the molecular level, and high resolution structures or mechanistic models are missing. More than 500 sequence entries are known, but few are functionally characterized in detail.

The first NAT to be sequenced and best studied eukaryotic member to date is UapA, a high affinity uric acid/xanthine:H<sup>+</sup> symporter from the ascomycote *Aspergillus nidulans* (4). Studies with chimeric transporter constructs, site-directed mutagenesis, second-site suppressors, and kinetic inhibition analysis of ligand specificity (5–8) have shown that a conserved NAT/NCS2 motif region between putative transmembrane helices VIII and IX of UapA includes determinants of substrate recognition and selectivity (8), with at least one residue (Gln-408) implicated in purine binding with the imidazole moiety of purines, whereas an aromatic residue at the middle of putative helix XII (Phe-528) may act as a substrate-selectivity filter to determine stringency of the purine translocation pathway (7, 9).

Recently, we have characterized the first purine-specific members of the NAT/NCS2 family from a Gram-negative bacterium, namely YgfO and YicE of *Escherichia coli* K-12 (10), as high affinity xanthine:H<sup>+</sup> symporters that cannot use uric acid, hypoxanthine, uracil, or other nucleobases as a substrate and cannot recognize analogues substituted at positions 7 or 8 of the imidazole ring (10, 11). We have also initiated a systematic series of Cys-scanning and site-directed mutagenesis studies of YgfO to elucidate structure-function relationships in a bacterial NAT (12). As part of these studies, we have shown that the NAT/NCS2-motif sequence region of YgfO includes essential determinants; Gln-324, irreplaceable for high affinity binding and uptake, Asn-325, irreplaceable for active transport, and an α-helical stripe of residues (Thr-332, Gly-333, Ser-336, Val-339), highly sensitive to site-directed alkylation and important for ligand specificity<sup>3</sup> (12). The studies also show that the bacterial (12) and fungal (8) NAT-motif determinants consent, implying that few residues conserved within the members of NAT family maybe invariably critical for function.

\* This paper is part of the 05NONEU547 research project, implemented within the framework of "Collaborations with Research and Technology Organizations outside Europe" and co-financed by National and Community Funds (25% from the Greek Ministry of Development, Secretariat for Research and Technology, and 75% from the European Union European Social Fund. The costs of publication of this article were defrayed in part by the payment of page charges. This article must therefore be hereby marked "advertisement" in accordance with 18 U.S.C. Section 1734 solely to indicate this fact.

<sup>3</sup> The on-line version of this article (available at <http://www.jbc.org>) contains supplemental Table S1.

<sup>1</sup> To whom correspondence should be addressed: University of Ioannina Medical School, Laboratory of Biological Chemistry, 45110 Ioannina, Greece. Tel.: 30-26510-97814; Fax: 30-26510-97868; E-mail: efriligo@cc.uoi.gr.

<sup>2</sup> The abbreviations used are: NAT (NCS2), nucleobase-ascorbate transporter; Cys-less (C-less), permease devoid of native Cys residues; HRP, horseradish

peroxidase; BAD, biotin-acceptor domain; NEM, *N*-ethylmaleimide; N<sub>11</sub>-C<sub>1</sub>, chimera containing sequence 1–419 of YgfO followed in-frame by sequence 505–547 of UapA and the C-terminus of YgfO-BAD; wt, wild type.  
<sup>3</sup> E. Georgopoulou and S. Frillingos, manuscript in preparation.

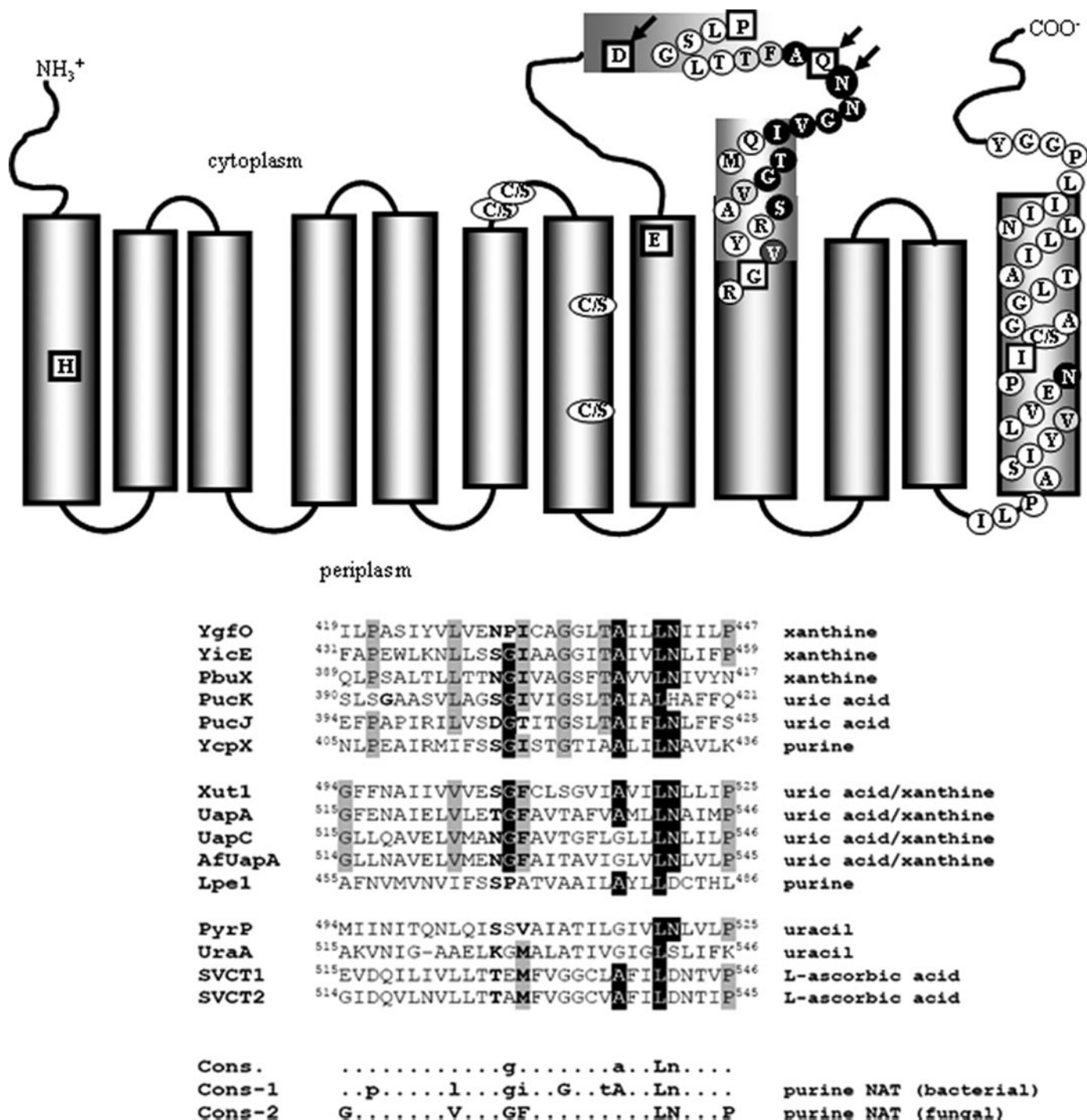
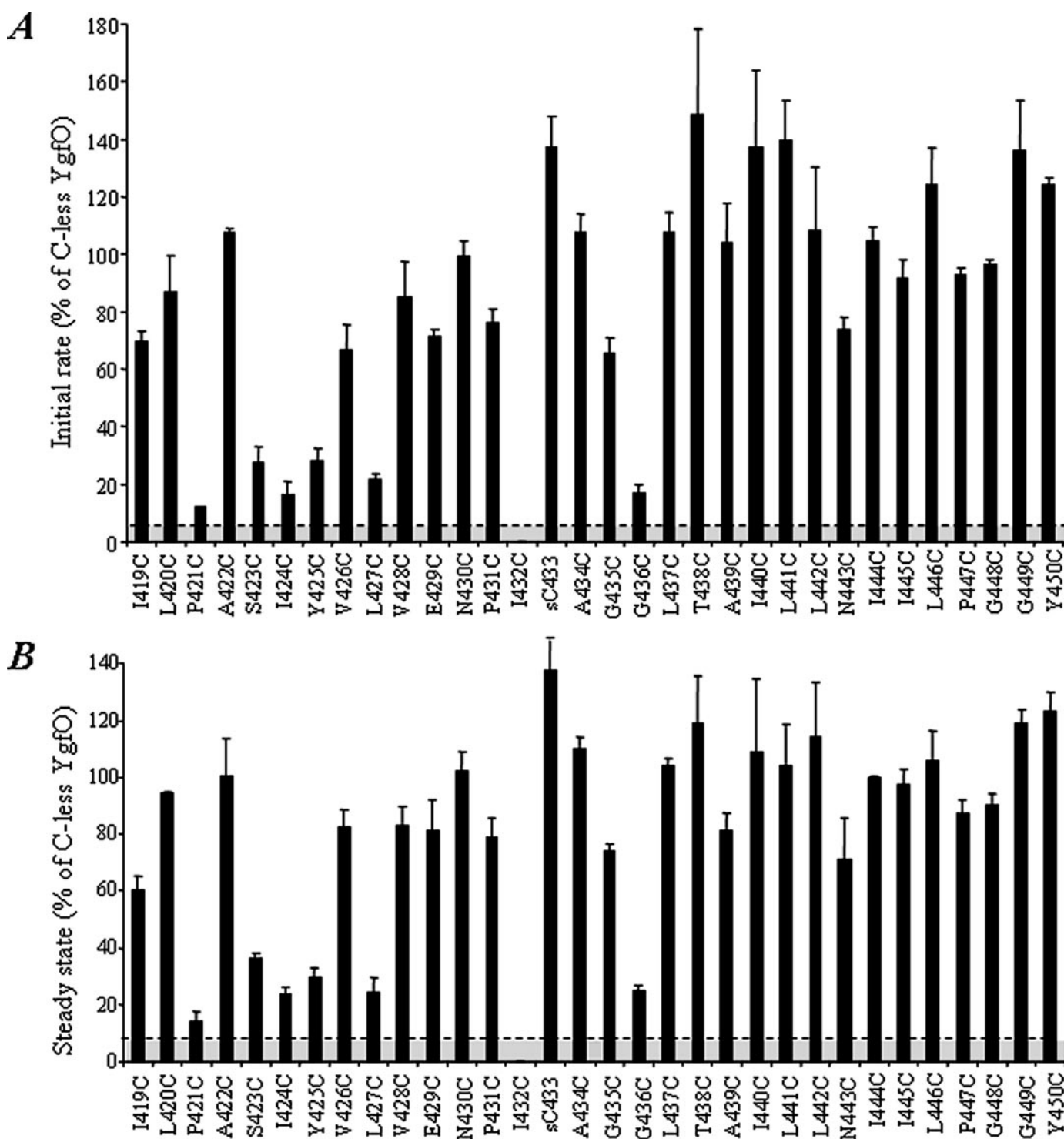


FIGURE 1. **Proposed topology and sequence alignment of helix XII and flanking regions of YgfO.** The topology diagram (upper panel) illustrates the location of sequence 419–450 in the context of the overall topological organization of YgfO. The model is based on program TMHMM, evidence that C terminus is cytoplasmic (10, 18), and our unpublished evidence (G. Mermelekas and S. Frillingos, manuscript in preparation) on the orientation of transmembrane helices 8–12. It also highlights the NAT-motif sequence region (12) and indicates irreplaceable residues (arrows), residues where one or more missense mutations yield negligible expression or activity (squares) (E. Karna and S. Frillingos, manuscript in preparation), and residues where a single-Cys is highly sensitive to inactivation by *N*-ethylmaleimide treatment (circled in a dark background). The five positions of native Cys residues that are replaced with Ser in the C-less background are indicated as C/S. The sequence alignment (lower panel) shows a consensus of the 15 characterized NAT/NCS2 transporters, including *E. coli* YgfO (P67444) (10), YicE (P0AGM9), and UraA (P0AGM7), *Bacillus subtilis* PbuX (P42086), PucK (O32140), and PucJ (O32139), *Clostridium perfringens* YcpX (BAB80103), *Lactococcus lactis* PyrP (AAK05701), *A. nidulans* UapA (Q07307) (8) and UapC (P487777), *Aspergillus fumigatus* AfUapA (XP748919) (23), *Candida albicans* Xut1 (AAX2221) (11), *Zea mays* Lpe1 (AAB17501) (24), *Homo sapiens* SVCT1 (SLC23A1) (AAH50261) and SVCT2 (SLC23A2) (Q9UGH3). The sequences were aligned using ClustalW. Residues similar to the consensus are shaded, and conservative substitutions are shown in lowercase.

An aromatic residue in the middle of putative helix XII of the fungal UapA (Phe-528) has been suggested to act as a substrate-selectivity filter to select against non-transported purines and

define stringency of the purine pathway but without participating in binding *per se* (9). Strikingly, sequences of helix XII are poorly conserved in NAT family, but Phe-528 is always con-



**FIGURE 2. Active xanthine transport activities of single-Cys mutants.** *E. coli* T184 harboring pT7-5/ygfO(C-less-BAD) with given mutations were grown aerobically at 37 °C in complete medium to mid-logarithmic phase, induced with isopropyl 1-thio- $\beta$ -D-galactopyranoside (0.5 mM) for 2 h, normalized to 0.7 mg of protein per ml of cell suspension, and assayed for transport of [ $^3$ H]xanthine (1  $\mu$ M) at 25 °C. *A*, initial rates of uptake were measured at 5–20 s. Control values obtained from T184 harboring pT7-5 alone (0.01 nmol mg $^{-1}$  min $^{-1}$  on average) were subtracted from the sample measurements in all cases. Results are expressed as a percentage of the rate of Cys-less YgfO (1.7 nmol mg $^{-1}$  min $^{-1}$  on average) with S.D. from three independent determinations. *B*, steady-state levels of xanthine accumulation (reached at 1–10 min for most mutants). Control values obtained from T184 harboring pT7-5 alone (0.01 nmol mg $^{-1}$  on average) were subtracted from the sample measurements in all cases. Results are expressed as a percentage of the level of Cys-less YgfO (0.8 nmol mg $^{-1}$  on average) with S.D. from three independent determinations.

served in fungal purine-transporting members, and an Ile is conserved at the corresponding position of bacterial purine-transporting NATs (Fig. 1). Thus, the bacterial YgfO, which has a distinct and more robust specificity with respect to position 8

of the imidazole ring (11), might not need a selectivity filter of the fungal type or use a different amino acid residue(s) as a selectivity filter outside helix XII (9). To initially address the role of helix XII in YgfO, we have replaced it with the corre-

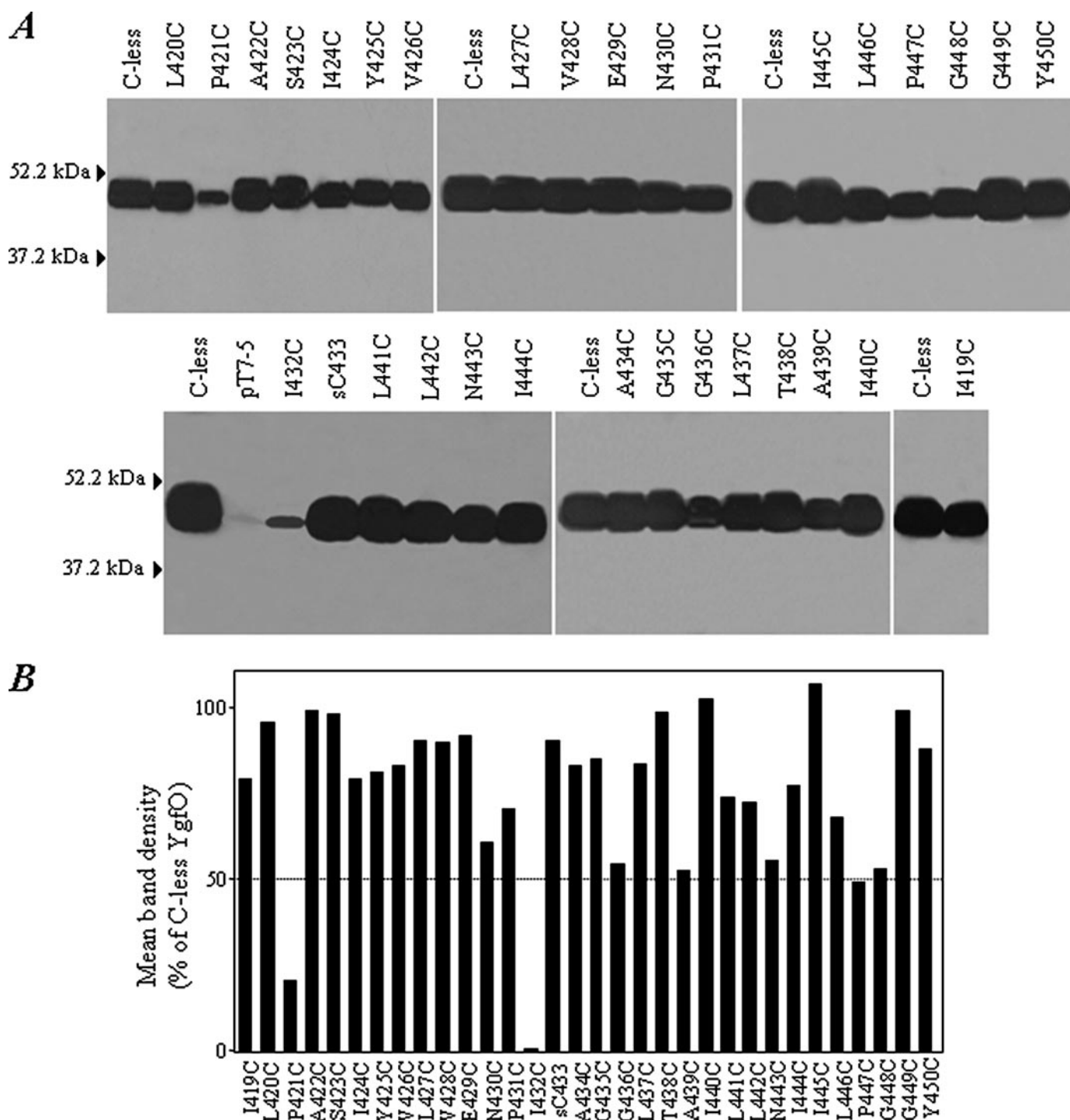


**FIGURE 3. Immunoblot analysis of single-Cys mutants.** Membranes were prepared from isopropyl 1-thio- $\beta$ -D-galactopyranoside-induced cultures of *E. coli* T184 harboring pT7-5/*ygfO*(C-less-BAD) with given mutations. Samples containing  $\sim 100 \mu\text{g}$  of membrane protein were subjected to SDS-PAGE (12%) and immunoblotting using HRP-conjugated avidin. Equivalent results were obtained when blots were re-probed with anti-LacY epitope antibody (not shown). A, representative blots of single-Cys mutants and Cys-less YgfO. Membranes prepared from cells harboring pT7-5 alone exhibited no immunoreactive material. Prestained molecular weight standards (Bio-Rad, low range) are shown on the left. B, quantitative estimation of the expression level of each mutant as a percentage of Cys-less expression derived from the relative density of the corresponding band. Results shown are the means of four determinations from two independent experiments, with S.D. that were  $< 15\%$ .

sponding segment of UapA (Fig. 1) to engineer chimera YgfO(N<sub>11</sub>)-UapA(C<sub>1</sub>) and found that the chimeric protein is expressed in the *Escherichia coli* membrane to decent levels but fails to catalyze active transport. This finding implies that the bacterial helix XII should also contain important determinants.

To analyze the role of helix XII more systematically, we have performed Cys-scanning and site-directed mutagenesis of sequence 419–450 of YgfO. Our combined evidence from transport, immunoblotting, sulfhydryl alkylation, and ligand inhibition assays of a set of 65 site-directed permease mutants

## Cys-scanning Analysis of YgfO Helix XII

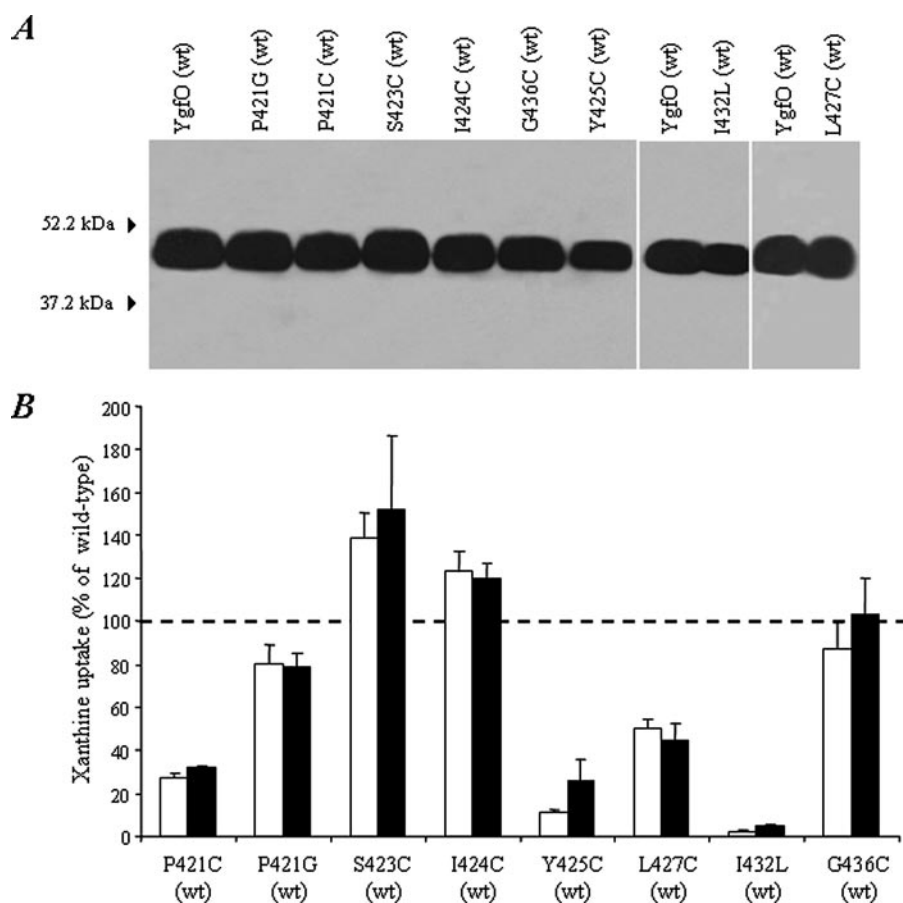


**FIGURE 4. Expression and xanthine uptake activities of Cys replacement and most-conservative-replacement mutants in the wild-type (wt) permease background.** *E. coli* T184 harboring pT7-5/ygfO(wild-type-BAD) with given mutations were grown, induced, and subjected to immunoblot analysis of membrane fractions (A) or assayed for transport of [<sup>3</sup>H]xanthine (1  $\mu$ M, 25 °C) (B and C) exactly as described in the legends to Figs. 2 and 3. Open and closed histogram bars in panel B represent initial rate and steady-state values, respectively, with S.D. shown from three independent experiments.

has shown that Asn-430 and Ile-432, in the approximate middle of helix XII, are crucial for function, and Asn-430 is probably at the vicinity of the purine binding site. Ile-432 aligns with Phe-528, the putative substrate-selectivity filter of UapA (9), and Asn-430 aligns with Thr-526, a residue that also appears to play a role in substrate selectivity.<sup>4</sup> The significance of our findings with respect to comparison with the major fungal NAT homolog (UapA) is discussed.

### EXPERIMENTAL PROCEDURES

**Materials**—[8-<sup>3</sup>H]Xanthine (27.6 Ci/mmol) was purchased from Moravex Biochemicals. Nonradioactive nucleobases and analogues were from Sigma. Oligodeoxynucleotides were synthesized from BioSpring GmbH. High fidelity Taq Polymerase (Expand High Fidelity PCR system) was from Roche Applied Science. Site-directed rabbit polyclonal antiserum against the C-terminal 12peptide of *E. coli* LacY was donated by H. R. Kaback (UCLA) and prepared by Berkeley Antibody Co., Inc. (Richmond, CA). Horseradish peroxidase (HRP)-conjugated penta-His antibody was from Qiagen. Avidin-HRP and protein A-HRP conjugates were from Amersham Biosciences. All other

<sup>4</sup> I. Papageorgiou and G. Diallinas, personal communication.

materials were reagent grade and were obtained from commercial sources.

**Bacterial Strains and Plasmids**—*E. coli* K-12 was transformed according to Inoue (13). TOP10F' (Invitrogen) was used for initial propagation of recombinant plasmids. T184 (14), harboring pT7-5/ygfO (10) with given replacements, was used for isopropyl 1-thio- $\beta$ -D-galactopyranoside-inducible expression from the *lacZ* promoter/operator. Plasmid pAN510 (9) (donated by G. Diallinas, Athens University) was used as a *uapA* template for the construction of YgfO-UapA chimeras (see below).

**DNA Manipulations**—Construction of expression plasmids and BAD-tagged versions of YgfO containing a C-terminal tail with the biotin-acceptor (BAD) domain of *Klebsiella pneumoniae* oxaloacetate decarboxylase and the C-terminal 12peptide of *E. coli* LacY has been described (10). Construction of His<sub>10</sub>-tagged versions, containing the C-terminal 12peptide of *E. coli* LacY followed in-frame by His<sub>10</sub> at the C terminus of YgfO has also been described (12). For construction of Cys-less YgfO, the five native-Cys codons were replaced simultaneously with Ser codons

using two-stage (multiple overlap/extension) PCR on the template of wild-type YgfO tagged at the C terminus with the BAD tag and subsequently transferred to the His<sub>10</sub>-tagged background by BamHI-HpaI restriction fragment replacement (12). For construction of Cys replacement mutants, two-stage (overlap/extension) PCR (15) was performed on the template of Cys-less YgfO tagged at the C terminus with either BAD or His<sub>10</sub> as indicated. Two-stage (overlap/extension) PCR using wild-type YgfO tagged at the C terminus with the BAD tag (10) and wild-type UapA (9) as templates was performed for the construction of chimeric YgfO-UapA proteins or combined replacement mutants as indicated. The entire coding sequence of all engineered constructs was verified by double-strand DNA sequencing in an automated DNA sequencer (MWG-Biotech).

**Growth of Bacteria**—*E. coli* T184 harboring given plasmids was grown aerobically at 37 °C in Luria-Bertani medium containing streptomycin (0.01 mg/ml) and ampicillin (0.1 mg/ml). Fully grown cultures were diluted 10-fold, allowed to grow to mid-logarithmic phase, induced with isopropyl 1-thio- $\beta$ -D-galactopyranoside (0.5 mM) for an additional 2 h at 37 °C, harvested, and washed with the appropriate buffers.

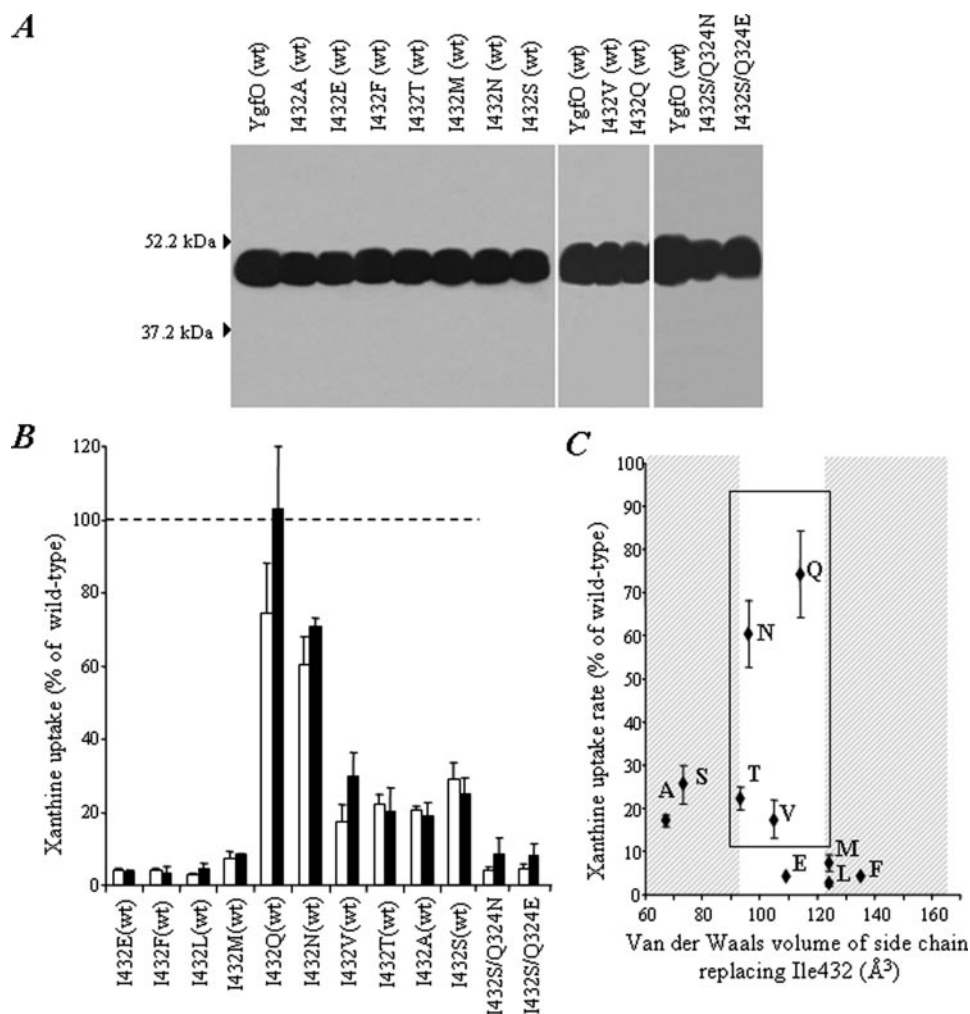


**FIGURE 5. Expression and xanthine uptake activities of site-directed mutants at position 432.** *E. coli* T184 harboring pT7-5/*ygfO* (wild-type-BAD) with given mutations were grown, induced, and subjected to immunoblot analysis of membrane fractions (A) or assayed for transport of [<sup>3</sup>H]xanthine (1  $\mu$ M, 25 °C) (B) exactly as described in the legends to Figs. 2 and 3. Open and closed histogram bars represent initial rate and steady-state values, respectively. C, correlation between mutant activity and van der Waals volume of side chain replacing Ile-432. wt, wild type.

**Transport Assays and Kinetic Analysis**—*E. coli* T184 were assayed for active transport of [<sup>3</sup>H]xanthine (1  $\mu$ M) by rapid filtration at both 25 and 37 °C, as described (10). For assaying the effect of *N*-ethylmaleimide (NEM), T184 cells were preincubated with NEM at the indicated conditions, reactions were stopped by the addition of a 20-fold excess of dithiothreitol, excess reagents and ligands were removed by centrifugation, and transport assays were performed in the presence of phenazine methosulfate (0.2 mM) and potassium ascorbate (20 mM) (16).

For ligand competition experiments, uptake of [<sup>3</sup>H]xanthine (1  $\mu$ M) was first assayed in the absence or presence of unlabeled analogues (1 mM), as described (12). For kinetic analysis, putative inhibitors were used in the concentration range of 0.1  $\mu$ M to 1 mM, and data were fitted to the appropriate equations using *Prism4*. IC<sub>50</sub> values were determined from full dose-response curves with a minimum of eight points spread over the relevant range. In all cases, the Hill coefficient was close to  $-1$ , consistent with presence of one binding site. In addition, we have examined the effect of analogues (1-methyl, 2-thio, and

8-methylxanthine) on  $K_m$  and  $V_{max}$  for wild-type and selected mutants and showed that  $V_{max}$  remains unaltered, consistent with competitive inhibition. This evidence suggests that a simple model of competition with the binding site of the transporter is applicable, satisfying the criteria for use of the Cheng and Prusoff equation  $K_i = IC_{50}/(1 + (L/K_m))$ , where  $L$  is the permeant concentration, and  $K_m$  is the value obtained for this permeant (11). It should be noted that the  $K_i$  value is an affinity constant implying binding to the transporter but does not indicate whether the ligand is being transported across the membrane.

**Immunoblot Analysis**—Membrane fractions of *E. coli* T184 harboring given plasmids were prepared and subjected to SDS-PAGE (12%) as described (10). Proteins were electroblotted to polyvinylidene difluoride membranes (Immobilon-PVDF; Pall Corp.). YgfO-BAD was probed with avidin-HRP or with a polyclonal antibody against the C terminus of *E. coli* LacY (17) followed by protein A-HRP. YgfO-His<sub>10</sub> was probed with penta-His antibody-HRP. Signals were developed with enhanced chemiluminescence (ECL).

**In Silico Analysis**—Comparative sequence analysis of NAT/NCS2 homologs was based on BLAST-p search and ClustalW alignment; the

most recent genome annotations were used for retrieving sequence data. Analysis of transmembrane topology was performed using program TMHMM (18).

## RESULTS

**Active Xanthine Transport**—Using a functional YgfO devoid of Cys residues (C-less), each amino acid residue in the sequence (Fig. 1) <sup>419</sup>ILPASIVLVENPICAGGLTAILLNILPGGY<sup>450</sup> including putative transmembrane helix XII (underlined) and flanking short segments was replaced individually with Cys. After verification of the sequence, each single-Cys mutant was transformed into *E. coli* T184 and assayed for its ability to catalyze active xanthine transport. As shown in Fig. 2A, of the 32 single-Cys mutants, 25 transport xanthine at rates that are between 60 and 150% of C-less permease, and 6 (P421C, S423C, I424C, Y425C, L427C, G436C) display low but significant uptake rates (10–25% of C-less). Mutant I432C displays a rate that approximates cells transformed with vector containing no *ygfO* insert. Steady-state levels of xanthine accumulation also show the same general picture

## Cys-scanning Analysis of YgfO Helix XII

(Fig. 2B); of the 32 single-Cys mutants, 25 accumulate xanthine to 80–130% of the steady state observed with C-less YgfO, 6 (P421C, S423C, I424C, Y425C, L427C, G436C) exhibit low levels (15–40% of C-less), and I432C is inactive.

**Expression in the Membrane**—Immunoblot analysis of BAD-tagged single-Cys permeases shows that low activity of mutant P421C and negligible activity of mutant I432C are associated with low expression in the membrane. All other mutants are expressed to high or moderate levels (Fig. 3).

**Expression and Transport Analysis of Mutants in Wild-type Background**—From the Cys-scanning transport analysis described above, few positions of inactive or low activity mutants were delineated. We analyzed these positions further by (a) transferring single-Cys mutations to the wild-type YgfO background and/or (b) engineering the most conservative site-directed replacement mutant to introduce an amino acid other than Cys. Thus, we constructed and assayed mutants (a) P421C(wt), S423C(wt), I424C(wt), Y425C(wt), L427C(wt), G436C(wt) and (b) P421G(wt) and I432L(wt) (Fig. 4). We found that S423C(wt), I424C(wt), G436C(wt), and P421G(wt) were highly active, L427C(wt) accumulated to 50% of wild type, and P421C(wt) and Y425C(wt) accumulated to low levels (15–30% of wild type), whereas I432L(wt) was inactive (Fig. 4B). All mutants of this set, including I432L(wt), are expressed in the membrane to high levels (Fig. 4A).

**Transport Analysis of Site-directed Mutants at Position 432**—Ile-432, where mutants with negligible activity had been detected (Figs. 2 and 4), was further subjected to extensive site-directed mutagenesis in the wild-type YgfO background. Site-directed mutants were initially analyzed for expression, active xanthine transport (Fig. 5), and kinetics of xanthine uptake (Table 1). Our data show that all mutants are expressed normally (Fig. 5A), but replacement of Ile-432 with Leu, Met, Glu, or Phe leads to inactivation, with Ala, Ser, Thr, or Val yields low activity (15–30%), and with Asn or Gln yields high activity (60–80%) (Fig. 5B). Clearly, decent uptake activity is permitted with a narrow window of side-chain volumes (95–125 Å<sup>3</sup>) and/or orientations at position 432 (Val, Glu, Leu, or Met yield activity <20%) (Fig. 5C). Kinetic analysis reveals that mutants with a small amino acid at position 432 (Ala, Ser) display a very low  $V_{\max}$ , whereas mutants with amino acids of intermediate bulk (Asn, Gln, Thr, Val) display  $V_{\max}$  approximating wild type and equivalent (Asn or Gln; 1.5-fold lower or 1.2-fold higher  $K_m$ ) or compromised affinities (Val or Thr; 4- or 3-fold higher  $K_m$ ). The most bulky replacements (Leu, Phe) display negligible uptake rates at any xanthine concentration tested (Table 1).

**Ligand Recognition Profiles of Site-directed Mutants at Position 432**—To understand whether Ile-432 contributes to the substrate and ligand recognition profile of YgfO, we assayed the active Ile-432 mutants for inhibition of [<sup>3</sup>H]xanthine uptake in the presence or absence of a series of purines and synthetic analogues (Table 2). When assayed in the presence of a 1000-fold molar excess of unlabeled antagonists, all Ile-432 mutants appear to follow the wild-type profile but with less efficient recognition of certain analogues, most notably 1-methylxanthine and 6-thioxanthine (Table 2). Kinetic analysis shows that mutants I432N(wt), I432V(wt),

**TABLE 1**  
 $K_m$  and  $V_{\max}$  values of YgfO mutants for xanthine uptake

*E. coli* T184 expressing the corresponding constructs were assayed for initial rates of xanthine uptake at 5–20 s in the concentration range of 0.1–100 μM; negative control values obtained from T184 harboring vector pT7-5 alone were subtracted from the sample measurements in all cases. Kinetic parameters were determined from non-linear regression fitting to the Michaelis-Menten equation using Prism4; values represent the means of three independent determinations with S.D. shown. All mutants as well as the wild-type YgfO version used in these experiments contained a C-terminal BAD. ND, assays were performed, but kinetic values were not determined due to very low uptake rates ( $\leq 0.05$  nmol mg<sup>-1</sup> min<sup>-1</sup>). Chimera YgfO(N<sub>11</sub>)-UapA(C<sub>1</sub>) is abbreviated as N<sub>11</sub>-C<sub>1</sub>.

Permease	$K_m$	$V_{\max}$	$V_{\max}/K_m$
	μM	nmol min <sup>-1</sup> mg <sup>-1</sup> protein	μl min <sup>-1</sup> mg <sup>-1</sup>
YgfO(wt)	4.6 ± 0.3	6.4 ± 0.5	1391
YgfO (C-less)	5.5 ± 0.5	10.2 ± 0.9	1858
<b>Single replacement mutants</b>			
I432A(wt)	1.6 ± 0.5	0.5 ± 0.1	313
I432S(wt)	1.8 ± 0.2	1.5 ± 0.2	833
I432N(wt)	2.6 ± 0.5	4.7 ± 0.2	1808
I432Q(wt)	5.0 ± 0.7	9.5 ± 0.4	1900
I432T(wt)	11.7 ± 1.5	5.7 ± 1.2	487
I432V(wt)	16.0 ± 3.4	5.4 ± 1.7	338
I432L(wt)	ND	ND	
I432F(wt)	ND	ND	
N430T(wt)	ND	ND	
I432L (C-less)	9.1 ± 0.7	12.1 ± 0.4	1330
N430C (C-less)	9.9 ± 1.8	23.1 ± 1.6	2333
<b>Double replacements</b>			
I432S(wt)	1.8 ± 0.2	1.5 ± 0.2	833
Q324N(wt)	76.0 ± 19.1	44.5 ± 4.7	586
I432S/Q324N(wt)	6.4 ± 2.7	3.6 ± 0.5	563
Q324E(wt)	71.2 ± 12.2	12.6 ± 0.4	177
I432S/Q324E(wt)	11.8 ± 3.9	4.4 ± 0.5	373
<b>Chimeric constructs</b>			
N <sub>11</sub> -C <sub>1</sub>	ND	ND	
N <sub>11</sub> -C <sub>1</sub> /F528I	ND	ND	
N <sub>11</sub> -C <sub>1</sub> /T526N	ND	ND	
N <sub>11</sub> -C <sub>1</sub> /T526N/F528I	3.8 ± 0.7	0.12 ± 0.01	32
N <sub>11</sub> -C <sub>1</sub> /T526N/G527P/F528I	1.5 ± 0.6	0.08 ± 0.01	53

and I432T(wt) display lower affinity (higher  $K_i$ ) for 1-methylxanthine (>25-fold), 6-thioxanthine (7.5-fold to >25-fold), and 3-methylxanthine (4-fold to 6.5-fold), similar or higher affinity for 2-thioxanthine and 9-methylxanthine, and no changes for the non-recognizable purines and substrate analogues (Table 3). Mutant I432Q(wt) also displays lower affinity (higher  $K_i$ ) for 1-methylxanthine (>25-fold) and 6-thioxanthine (10-fold), slightly higher affinity for 2-thioxanthine or 3-methylxanthine, and no changes for the other analogues (Table 3).

**Ile-432 Replacements in the C-less Background**—To examine whether the native Cys residue Cys433 (Fig. 1) affects the properties of Ile-432 mutants, we also engineered a series of mutants at position 432 in the C-less background containing Ser-433 (Fig. 6). In this background all mutants except I432C (Fig. 3) are expressed normally (Fig. 6A), but replacement of Ile-432 with most bulky side chains (Phe, Trp) inactivates YgfO completely, replacement with equally or slightly less bulky side chains leads to intermediate (Leu; 55–70%) or low uptake activity (Met, Gln; 20–30%), and replacement with small side chains (Ser, Ala) leads to very low activity (rates, 10–15% of C-less). The most active mutant of this set, I432L(C-less), was further assayed for xanthine transport kinetics (Table 1) and ligand recognition in competitive inhibition experiments (Table 3) and found to display normal  $V_{\max}$  with compromised transport affinity (1.6-fold higher

TABLE 2

## Specificity profile of YgfO mutants at position 432 of helix XII

Values shown express % of [<sup>3</sup>H]xanthine (1 μM) uptake rate in the presence of a 1000-fold excess (1 mM) of unlabeled competitors. The uptake value obtained in the absence of competitor was taken as 100%. Values represent the means of at least three determinations; S.D. were always <20%. Most significant differences from the wild-type profile are highlighted in bold. All mutants as well as the wild-type version used in these experiments contained a C-terminal BAD. Although not shown, the specificity profile of C-less YgfO is indistinguishable from the one of wild type, except for a marginal ability to recognize 7-methyl and 8-methylxanthine (rate retained, 36–40%).

Competitor	Single replacements, [ <sup>3</sup> H]Xanthine uptake rate retained							
	wt	I432Q	I432N	I432V	I432T	I432S	I432A	I432L (C-less)
	%							
None	100	100	100	100	100	100	100	100
Uric acid	97	87	76	65	62	68	70	75
Hypoxanthine	96	80	114	90	81	95	73	74
Adenine	96	92	154	102	87	109	72	90
Guanine	94	86	86	105	99	100	62	71
Uracil	101	96	156	92	108	101	76	95
1-Methylxanthine	19	<b>63</b>	<b>67</b>	<b>76</b>	<b>78</b>	<b>53</b>	<b>54</b>	<b>75</b>
2-Thioxanthine	13	18	12	18	25	37	21	25
3-Methylxanthine	25	30	44	72	<b>79</b>	<b>60</b>	32	10
6-Thioxanthine	20	<b>56</b>	<b>36</b>	<b>65</b>	<b>85</b>	52	47	47
7-Methylxanthine	105	75	88	78	83	73	66	50
8-Methylxanthine	96	<b>40</b>	66	87	92	156	<b>26</b>	51
9-Methylxanthine	13	15	12	28	<b>36</b>	<b>39</b>	53	24
Allopurinol	106	81	119	75	80	83	54	82
Oxypurinol	31	5	12	36	44	33	17	4

Competitor	Double replacements, [ <sup>3</sup> H]Xanthine uptake rate retained					
	wt	I432S	Q324N	I432S/Q324N	Q324E	I432S/Q324E
	%					
None	100	100	100	100	100	100
Uric acid	97	68	143	99	122	78
Hypoxanthine	96	95	125	100	90	<b>33</b>
Adenine	96	109	90	142	124	<b>65</b>
Guanine	94	100	97	64	80	45
Uracil	101	101	128	103	98	86
1-Methylxanthine	19	53	<b>90</b>	<b>92</b>	<b>93</b>	<b>63</b>
2-Thioxanthine	13	37	<b>123</b>	<b>98</b>	<b>113</b>	57
3-Methylxanthine	25	<b>60</b>	79	<b>69</b>	<b>85</b>	41
6-Thioxanthine	20	52	<b>61</b>	<b>68</b>	50	<b>125</b>
7-Methylxanthine	105	73	69	74	112	66
8-Methylxanthine	96	156	70	75	75	78
9-Methylxanthine	13	39	<b>117</b>	<b>110</b>	<b>92</b>	28
Allopurinol	106	83	105	91	124	<b>62</b>
Oxypurinol	31	33	<b>69</b>	57	<b>62</b>	18

TABLE 3

## Kinetics of competitive inhibition for the most active I432 replacement YgfO mutants

Most significant differences from YgfO(wt) are highlighted in bold. Competition assay and kinetic analysis were performed as described under "Experimental Procedures." Values with S.D. shown represent the means of three determinations. Mutants used contained a C-terminal BAD.

Competitor	$K_i$					
	YgfO(wt)	I432Q(wt)	I432N(wt)	I432V(wt)	I432T(wt)	I432L(C-less)
	μM					
Uric acid	>1000	>1000	>1000	>1000	>1000	>1000
1-Methylxanthine	36	<b>&gt;1000</b>	<b>&gt;1000</b>	<b>&gt;1000</b>	<b>&gt;1000</b>	<b>&gt;1000</b>
2-Thioxanthine	91	42	31	8	16	79
3-Methylxanthine	72	<b>18</b>	314	<b>460</b>	471	<b>306</b>
6-Thioxanthine	41	<b>416</b>	<b>301</b>	<b>941</b>	>1000	<b>798</b>
7-Methylxanthine	>1000	>1000	>1000	>1000	>1000	>1000
8-Methylxanthine	>1000	833	>1000	>1000	>1000	>1000
9-Methylxanthine	53	38	76	9	10	159

$K_m$  than C-less) and lower affinity (higher  $K_i$ ) for recognition of 1-methylxanthine (>25-fold), 6-thioxanthine (20-fold), and 3-methylxanthine (4-fold). Overall, properties of Ile-432 mutants in the C-less background show the same trends as in the wild-type background (inactivation with very bulky replacements, 55–80% activity but with compromised  $K_m$  and/or poor affinity for certain analogues with replacements of intermediate bulk, low activity with smaller replacements), but the window of side-chain volumes that permits decent uptake activity is shifted to the right (110–130 Å<sup>3</sup>) (Fig. 6C).

*Functional Interaction of Ile-432 with the NAT Motif Region*—The NAT motif region of YgfO contains residues essential for high-affinity binding and uptake and for refinement of ligand specificity (12). In the homologous fungal UapA, the NAT motif has been proposed to directly bind at the imidazole moiety of substrate through Gln-408 (8) and act synergistically with Phe-528, the putative selectivity filter of helix XII, to allow stringency of the purine translocation pathway (9). To examine whether a similar interaction between helix XII and the NAT motif exists in YgfO, we engineered double-replacement mutants that combine I432S (helix XII), a

## Cys-scanning Analysis of YgfO Helix XII

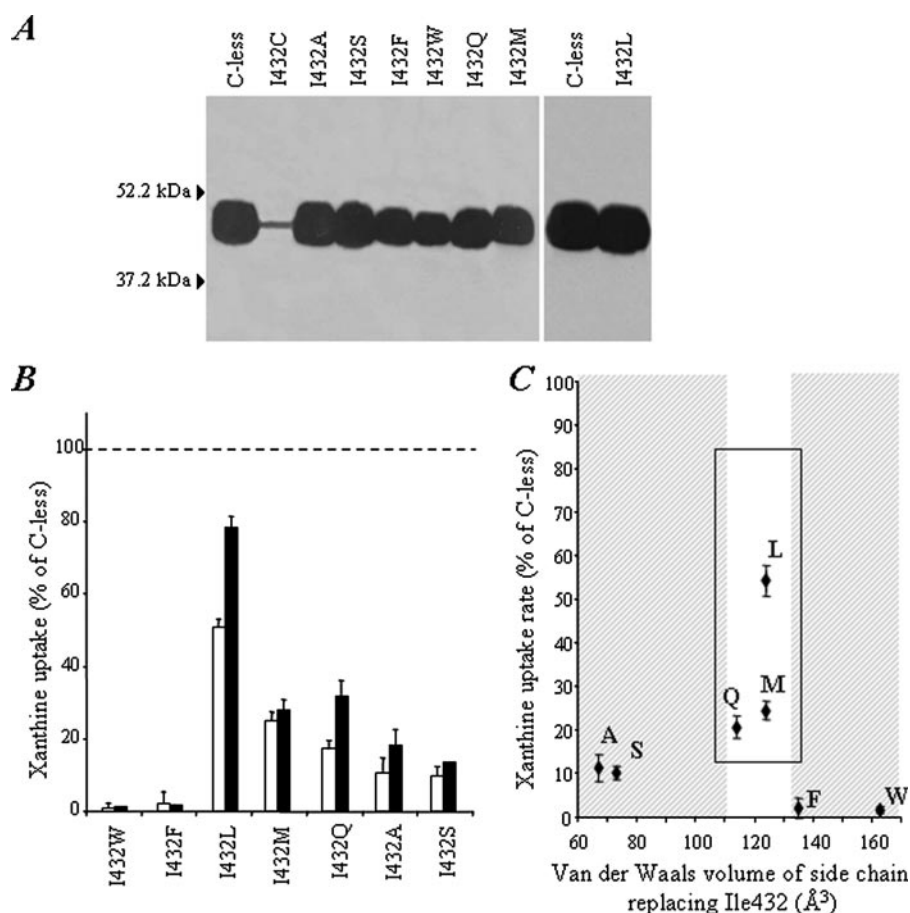


**FIGURE 6. Expression and xanthine uptake activities of site-directed mutants at position 432, constructed in the C-less permease background.** *E. coli* T184 harboring pT7-5/ygfO(C-less-BAD) with given mutations were grown, induced, and subjected to immunoblot analysis of membrane fractions (A) or assayed for transport of [<sup>3</sup>H]xanthine (1  $\mu$ M, 25  $^{\circ}$ C) (B), exactly as described in the legends to Figs. 2 and 3. Open and closed histogram bars represent initial rate and steady-state values, respectively. C, correlation between mutant activity and van der Waals volume of the side chain replacing Ile-432.

mutation leading to low uptake and poor recognition of certain analogues, with Q324N or Q324E (motif region), mutations leading to very low transport affinity and impaired binding for all analogues (12). Interestingly, both combinatorial mutants display normal expression in the membrane (Fig. 5) and low transport activity (Fig. 5) but without major impairment in transport affinity (Table 1). In addition, I432S/Q324E allows binding of 9-methylxanthine, oxypurinol and, less efficiently, 2-thioxanthine or 3-methylxanthine, analogues that are not recognized by Q324E (Table 2). Finally, I432S/Q324E displays an unprecedented, novel property to recognize non-xanthine purines (hypoxanthine, adenine, and guanine) (Table 2). Active transport assay for the uptake of [<sup>3</sup>H]hypoxanthine (10) showed that neither I432S/Q324E nor any of the parental mutants (I432S or Q324E) can take up hypoxanthine at concentrations 1–100  $\mu$ M (data not shown).

**Effect of N-Ethylmaleimide on Transport Activity**—The effect of NEM, a membrane-permeable sulfhydryl reagent, on the initial rate of xanthine transport for each single-Cys mutant is presented in Fig. 7. When incubated with 2 mM NEM (Fig. 7A), it is found that only three single-Cys are inhibited significantly, N443C by 50%, V426C by 70%, and N430C by 85%, activity of I427C is increased 1.4-fold, and activity of the remaining sin-

gle-Cys mutants is essentially unaltered (<1.2-fold enhancement or inhibition). V426C, N430C, and N443C were then assayed in the concentration range of 5  $\mu$ M to 2 mM, and the concentration resulting in 50% reduction of initial rate (IC<sub>50</sub>) was determined. As shown in Fig. 7B, N430C is highly sensitive to NEM (IC<sub>50</sub>, 10  $\mu$ M), whereas V426C, falling on the same face of an  $\alpha$ -helix in the periplasmic half of helix XII, is moderately sensitive (IC<sub>50</sub>, 0.4 mM), and N443C displays low sensitivity (IC<sub>50</sub>, 2 mM).

**N430C Alkylation Interferes with Ligand Binding**—The highly NEM-sensitive N430C was assayed for the effect of xanthine and xanthine analogues on the inactivation attained with NEM (Fig. 7C). Initial experiments using xanthine (1 mM) yielded no significant effects on the N430C inactivation rate (data not shown), but this was probably related to the fact that xanthine is transported and would, therefore, occupy the binding site for a shorter time than a high affinity non-transportable analogue; solubility limitations (8, 10) did not allow us use xanthine at concentrations >1 mM. We next focused attention on the effects of putative high affinity xanthine analogues. It was found that

2-thioxanthine (1 mM), an analogue that competes with xanthine for high affinity binding ( $K_i$  9  $\mu$ M), protects N430C against inactivation completely (Fig. 7C). At the same conditions, analogues that are poorly recognized by N430C ( $K_i$  > 0.5 mM) protect partially (6-thioxanthine) or offer no detectable protection (1-, 3-, or 9-methylxanthine) (not shown). When used in dose-response experiments, 2-thioxanthine was found to protect N430C with an EC<sub>50</sub> of 0.15 mM (Fig. 7C).

**Mutant N430T Is Inactive**—Although replacement of Asn-430 with Cys retains high activity (Fig. 2) but with poor affinity for several xanthine analogues (Table 2), replacement of Asn-430 with Thr in the wild-type background inactivates the permease completely (Table 1).

**Both Ile-432 and Asn-430 Are Needed to Rescue Activity of Chimera YgfO(N<sub>11</sub>)-UapA(C<sub>1</sub>)**—The chimeric protein YgfO(N<sub>11</sub>)-UapA(C<sub>1</sub>) or N<sub>11</sub>-C<sub>1</sub> (Fig. 8) engineered by replacing the sequence of YgfO helix XII (420–451) with the corresponding segment of UapA (505–547) was found to express in the *E. coli* membrane, albeit to low levels, but catalyze negligible active transport. Based on the Cys-scanning analysis, two residues of YgfO helix XII appear to be critical, Ile-432 and Asn-430. When replaced individually with the corresponding amino acid found in UapA, mutant I432F or N430T displays normal

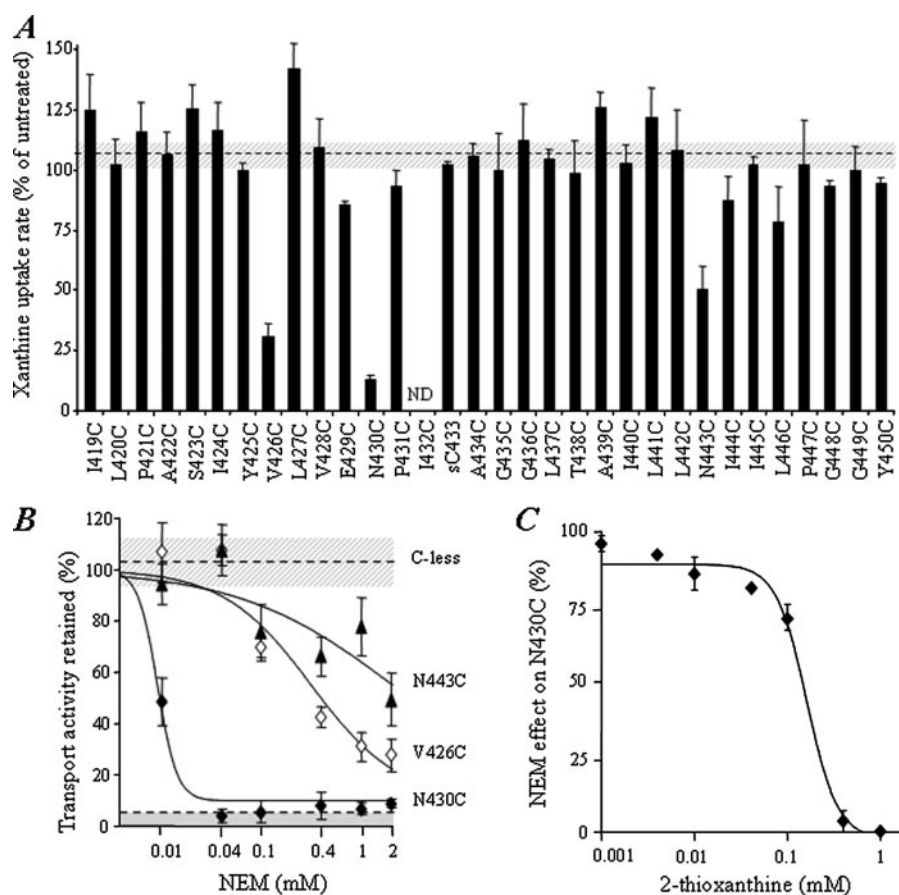


**FIGURE 7. Effect of NEM on the xanthine transport activity of single-Cys mutants.** *E. coli* T184 harboring pT7-5/ygfO(C-less-BAD) with given mutations were grown, induced, and assayed for transport of [ $^3$ H]xanthine (1  $\mu$ M, 25  $^{\circ}$ C). Cells had been preincubated in the absence or presence of either 2 mM NEM (A) or a range of NEM concentrations (5  $\mu$ M, 10  $\mu$ M, 20  $\mu$ M, 40  $\mu$ M, 0.1 mM, 0.4 mM, 1 mM, 2 mM) (B) for 10 min at 25  $^{\circ}$ C. Transport assays were performed in the presence of 20 mM potassium ascorbate and 0.2 mM phenazine methosulfate. A, effect of 2 mM NEM. Rates are presented as percentages of the rate measured in the absence of NEM with S.D. from three independent determinations shown. Average and S.D. values of C-less control are also shown as *dashed line* and *gray horizontal bars*, respectively. Values were not determined (ND) for mutant I432C, which displays negligible initial rate. B, NEM dose-response curves for mutants V426C, N430C, and N443C. IC<sub>50</sub> values were deduced from these data using the *Prism4* software. C, effect of substrate on the inactivation of N430C attained with NEM. Incubation with NEM (0.1 mM) in the absence or presence of 2-thioxanthine (1  $\mu$ M, 4  $\mu$ M, 10  $\mu$ M, 40  $\mu$ M, 0.1 mM, 0.4 mM, 1 mM) was followed by removal of excess reagent and ligand by centrifugation before transport assay. The inactivation effects were calculated as deviations of each uptake rate from the rate measured in the absence of NEM and presented as percentages of the inactivation effect of NEM in the absence of ligand. Values with S.D. from three independent determinations are shown.

expression in the membrane but zero activity (see above). We re-introduced Ile-432/528 and/or Asn-430/526 in the background of chimera N<sub>11</sub>-C<sub>1</sub> to test whether these two residues of helix XII can restore function. Normal expression is restored, and significant xanthine uptake activity is rescued with the double mutant N<sub>11</sub>-C<sub>1</sub>/T526N/F528I but not with either one of N<sub>11</sub>-C<sub>1</sub>/T526N or N<sub>11</sub>-C<sub>1</sub>/F528I (Fig. 8). Significant uptake activity is also rescued with N<sub>11</sub>-C<sub>1</sub>/T526N/G527P/F528I, in which, apart from T526N and F528I, the intervening residue (Gly) has also been replaced with the one found in YgfO (Pro) (Fig. 8). Kinetics and ligand inhibition analysis of the two active chimeras reveals that their transport affinity for xanthine is at least as high as the one of wild-type YgfO, but their V<sub>max</sub> is low (2% of wild-type) (Table 1), and the ligand specificity profile differs from the one of wild-type YgfO, showing less efficient recognition of 1-methyl and 9-methylxanthine and a striking

ability to bind analogues modified at purine positions 7 or 8 that are not or are poorly bound by wild type (7- or 8-methylxanthine, oxypurinol) (Fig. 8C).

## DISCUSSION

We have studied the role of putative transmembrane helix XII of the NAT family by Cys-scanning and site-directed mutagenesis in the major xanthine-specific bacterial homolog YgfO and found that Asn-430 and Ile-432, at the approximate middle of transmembrane helix XII, are important for the permease function. Although replaceable, these two residue positions appear to pose specific steric constraints to substrate or substrate analogue binding, leading to the observed phenotypes of site-directed mutants with impaired activity or low affinity for xanthine transport and/or binding of bulky replacement analogues. Steric constraints probably represent direct effects in the case of Asn-430, based on the site-directed alkylation experiments (Fig. 7), but are probably exerted through indirect interactions in the case of Ile-432, which is on the opposite side of the helix (Fig. 9). In any case, Asn-430 or Ile-432 *per se* or the relative polar character of the amino acid group at each position is replaceable for transport, excluding the possibility of direct participation in xanthine binding through specific hydrophobic (Ile) or hydrogen-bonding interactions (Asn).

With respect to Asn-430, our finding that single-Cys N430C is sensitive to inactivation by *N*-ethylmaleimide (IC<sub>50</sub>, 10  $\mu$ M) and completely protected against inactivation by a high affinity substrate analogue (2-thioxanthine) implies that this residue is close to the purine binding site. The observation that the physiological YgfO substrate, xanthine, offers no detectable protection at similar concentrations ( $\leq$  1 mM) may mean that binding affinity for xanthine is lower and/or reflects the high uptake capacity, which lowers the effective xanthine concentration at the binding site. In another paradigm of secondary active transporter, a very similar mutant behavior, *i.e.* high activity, sensitivity to inactivation by site-directed alkylation, and complete protection in the presence of a high affinity ligand but less efficient protection by substrate itself, had been described for Cys-148 in the lactose permease of *E. coli* (19), and this residue was indeed found to be vicinal to the binding site by x-ray crystallography (20, 21).

## Cys-scanning Analysis of YgfO Helix XII

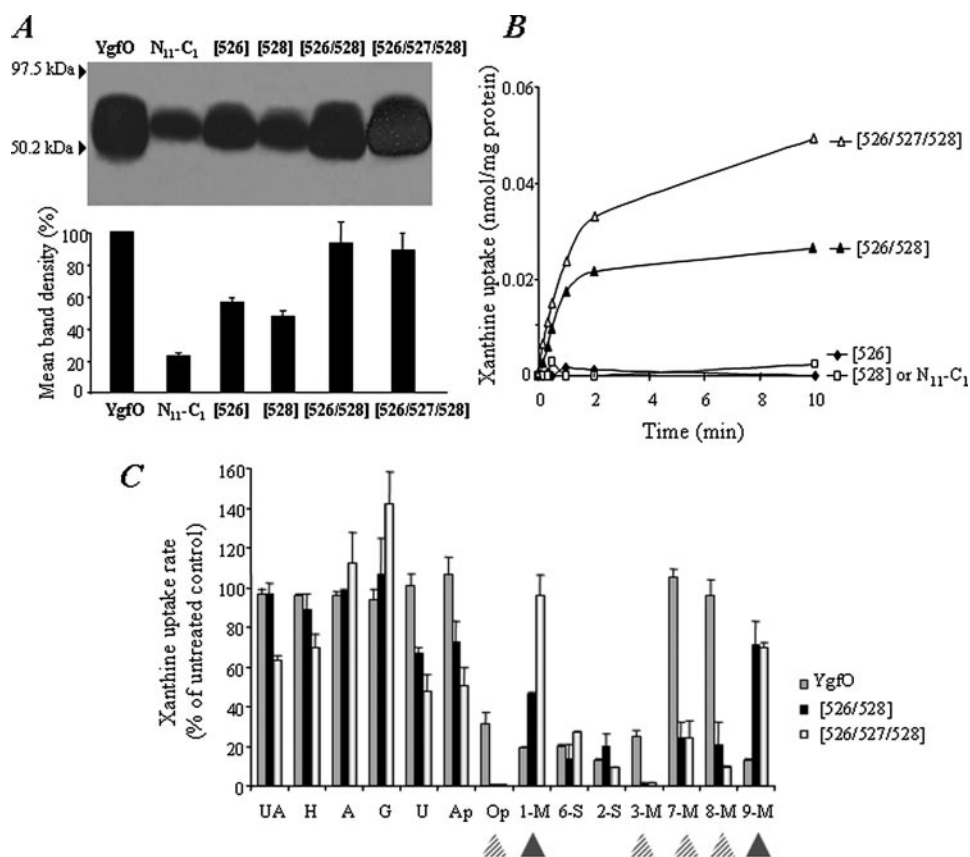


**FIGURE 8. Expression, xanthine uptake activities, and ligand recognition properties of YgfO-UapA cross-homolog chimeras with replacements at helix XII.** *E. coli* T184 harboring pT7-5/ygfO(wild-type-BAD) with sequence 420–451 replaced with codon sequence 505–547 from UapA (chimera  $N_{11-C_1}$ ), and given mutations were grown, induced, and subjected to immunoblot analysis of membrane fractions (A) or assayed for transport of [ $^3$ H]xanthine ( $1 \mu\text{M}$ ,  $25^\circ\text{C}$ ) (B), as described in the legends to Figs. 2 and 3. The active chimera mutants were also subjected to ligand-competition transport analysis (C), as described in the legend to Table 2. A, representative immunoblots and quantitative estimation of the expression level of each construct as a percentage of wild-type YgfO expression derived from the relative density of the corresponding band. Results with S.D. shown are the means of three independent determinations. B, active transport assays for chimera  $N_{11-C_1}$  and mutants thereof. C, ligand recognition profiles of the active chimera mutants. Values shown express % of [ $^3$ H]xanthine ( $1 \mu\text{M}$ ) uptake rate in the presence of a 1000-fold excess (1 mM) of unlabeled competitors and represent the means of three determinations with S.D. shown. The unlabeled nucleobases and analogues used are: UA, uric acid; H, hypoxanthine; A, adenine; G, guanine; U, uracil; Ap, allopurinol; Op, oxypurinol; 1-M, 1-methylxanthine; 6-SX, 6-thioxanthine; 2-MX, 2-methylxanthine; 3-MX, 3-methylxanthine; 7-MX, 7-methylxanthine; 8-MX, 8-methylxanthine; 9-MX, 9-methylxanthine. The chimera constructs are abbreviated as follows:  $N_{11-C_1}$ , YgfO( $N_{11}$ )-UapA( $C_1$ ) i.e. chimera containing sequence 1–419 of YgfO followed in-frame by sequence 505–547 of UapA and the C terminus of YgfO-BAD; [526], chimera  $N_{11-C_1}$  with mutation T526N; [528], chimera  $N_{11-C_1}$  with mutation F528I; [526/528], chimera  $N_{11-C_1}$  with mutations T526N/F528I; [526/527/528], chimera  $N_{11-C_1}$  with mutations T526N/G527P/F258I.

With respect to Ile-432, which is probably situated on the other side of the  $\alpha$ -helix but at the same depth in the membrane as Asn-430 (Fig. 9), our extensive mutagenesis data suggest that it may affect constraints in the purine binding site indirectly. A bulkier or differently oriented side chain at this position is refractory for substrate insertion or translocation possibly due to steric confluence and unfavorable rearrangement of helices that is transmitted to Asn-430 in the binding pocket. For the same reason, a smaller side chain may allow xanthine binding and transport, even with reduced affinity, but hinder recognition of bulky substituents at the pyrimidine moiety of substrate, leading to the observed impairment of binding for 1-methyl and 6-thioxanthine.

Although conservation of the sequence of putative transmembrane helix XII among NAT transporters is poor, it is

notable that a hydrogen-bonding amino acid (mostly Asn, Thr, or Ser) is conserved at the position of residue Asn-430 and a hydrophobic amino acid (mostly Ile, Phe, or Met) at the position of residue Ile-432, with Gly or Pro at the intervening position of purine transporters (Fig. 1). In the homologous sequence of the fungal UapA transporter, Ile-432 and Asn-430 align with Phe-528 and Thr-526, respectively. It is interesting to note that Phe-528 in UapA has been proposed to act as a substrate-selectivity filter that synergizes with but is distinct from the purine binding site (9). The authors base their proposal on the finding that replacement of the aromatic ring at this position results in low affinity uptake of novel purine substrates such as hypoxanthine and guanine but without impairing the normal transport activity for the physiological substrates (uric acid, xanthine, oxypurinol) (7, 9). Replacement of Thr-526 with Ala was also shown to affect substrate selectivity.<sup>4</sup> Thus, in both the bacterial and the fungal homolog, the two residues of helix XII (Ile/Phe and Asn/Thr) appear to serve a critical role associated with optimal stringency for purine binding and/or translocation. The role, however, is much more crucial in the bacterial YgfO, where recognition of substrate and substrate analogues is subject to more steric constraints than in the fungal UapA (10, 11).

On line with the above, properties of the mutants in both YgfO and UapA imply that the median part of

transmembrane helix XII containing Ile/Phe-432 and Asn/Thr-430 is close to the binding site in the tertiary structure. In YgfO, this contention is strongly supported by our finding that ligand binding can protect N430C from inactivation with *N*-ethylmaleimide. In UapA, such information is not available, but it is suggested that Phe-528 interacts with Gln-408, a residue implicated with purine binding (8), based on the functional properties of a series of double mutants (9). Because Gln-408 (Gln-324 in YgfO) is highly conserved in the NAT motif sequence region (Fig. 1) and appears to play a critical and finely tuned role in purine binding in both the bacterial YgfO and the fungal UapA system (8, 12), it is reasonable to assume that an interaction between Gln-324 (motif) and Ile-432 (helix XII) also exists in YgfO. Initial evidence for such an interaction is provided from our double

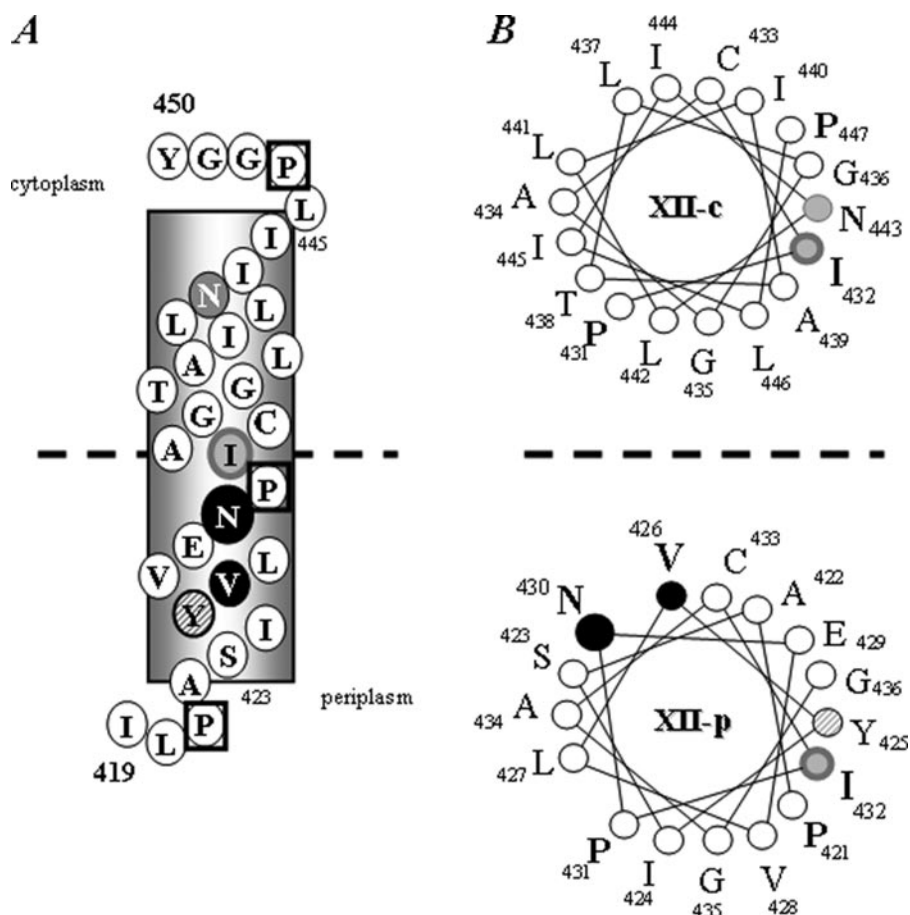


**FIGURE 9. Secondary structure model of putative transmembrane helix XII of YgfO permease (A) and  $\alpha$ -helical wheel plots of residues 431–447 (cytoplasmic half, XII-c) and residues 421–436 (periplasmic half, XII-p) (B).** The approximate middle of the helix is indicated by the bold dashed line. The three Pro residues (421, 431, and 447) are boxed. Residues sensitive to inactivation of a single-Cys by *N*-ethylmaleimide (Asn-430, Val-426, Asn-443) (Fig. 7) as well as Ile-432 (Fig. 5) are highlighted in a dark background. Residue Tyr-425, yielding low activity of a Cys mutant (Fig. 4), is cross-hatched.

mutant experiments (Tables 1 and 2), showing that the impaired-affinity properties of Q324E (12) are ameliorated in the background of I432S/Q324E mutant, and novel properties arise namely to recognize non-xanthine purines (adenine, guanine, hypoxanthine). Similar observations have been made with mutant F528S/Q408E in UapA (7, 9). To analyze further the putative spatial proximity between the NAT motif region and the important residues of helix XII, additional studies are needed using double-Cys mutants and cross-linking experiments. Such studies are under way in our laboratory.

Finally, it was examined whether the two important residues of YgfO helix XII (Asn-430 and Ile-432) can rescue activity in an inactive cross-homolog chimera where the entire sequence of helix XII is conferred by the fungal UapA, whereas the rest of the protein derives from YgfO (chimera  $N_{11}$ - $C_1$ ) (Fig. 8). Reintroduction of an Asn or an Ile alone in place of Thr-526 or Phe-528, respectively, improves expression of the  $N_{11}$ - $C_1$  chimera but fails to rescue any activity. Combinatorial replacement of both Thr-526 and Phe-528 with Asn and Ile, respectively, in the median sequence region of helix XII restores normal expression in the *E. coli* membrane and rescues significant xanthine uptake activity but

with striking deviations from the ligand specificity profile of wild-type YgfO. Most importantly, xanthine analogues modified at positions 7 or 8 (7-methyl or 8-methylxanthine or oxypurinol) are now clearly recognized, implying that steric constraints for binding at the imidazole moiety of purine (10–12) are released in the chimeric  $N_{11}$ - $C_1$  background. This is possibly due to other amino acid determinants of helix XII that differ between YgfO and UapA (Fig. 1) or to different orientations of Asn-430 and/or Ile-432 with respect to the bound substrate or with respect to other interacting protein regions such as the NAT motif in the background of the  $N_{11}$ - $C_1$  chimera. In any event, it appears that the purine binding site of YgfO is genetically flexible, and relatively few amino acid changes can lead to binding of novel substrate analogues that are not recognized by wild type. A similar contention has been reached from the work on the fungal transporter UapA (7–9, 22, 23).<sup>4</sup> Taken together, the ongoing research on the bacterial (YgfO) and the fungal (UapA) NAT prototypes is expected to provide important insights on the mechanism and evolution of purine substrate selectivity and ligand

specificity in this ubiquitous and highly conserved family of nucleobase-ascorbate transporters.

*Acknowledgments*—We thank George Diallinas and H. Ronald Kaback for helpful discussions, Panayiota Karatza for mutant C433S(wt), and Sotiria Libanovnou for construction of mutant I419C.

## REFERENCES

1. Tsukaguchi, H., Tokui, T., Mackenzie, B., Berger, U. V., Chen, X. Z., Wang, Y., Brubaker, R. F., and Hediger, M. A. (1999) *Nature* **399**, 70–75
2. de Koning, H., and Diallinas, G. (2000) *Mol. Membr. Biol.* **17**, 75–94
3. Liang, W. J., Johnson, D., and Jarvis, S. M. (2001) *Mol. Membr. Biol.* **18**, 87–95
4. Diallinas, G., and Scazzocchio, C. (1989) *Genetics* **122**, 341–350
5. Diallinas, G., Valdez, J., Sophianopoulou, V., Rosa, A., and Scazzocchio, C. (1998) *EMBO J.* **17**, 3827–3837
6. Meintanis, C., Karagouni, A. D., and Diallinas, G. (2000) *Mol. Membr. Biol.* **17**, 47–57
7. Amillis, S., Koukaki, M., and Diallinas, G. (2001) *J. Mol. Biol.* **313**, 765–774
8. Koukaki, M., Vlanti, A., Goudela, S., Pantazopoulou, A., Gioule, H., Tournaviti, S., and Diallinas, G. (2005) *J. Mol. Biol.* **350**, 499–513
9. Vlanti, A., Amillis, S., Koukaki, M., and Diallinas, G. (2006) *J. Mol. Biol.* **357**, 808–819
10. Karatza, P., and Frillingos, S. (2005) *Mol. Membr. Biol.* **22**, 251–261
11. Goudela, S., Karatza, P., Koukaki, M., Frillingos, S., and Diallinas, G. (2005)

## Cys-scanning Analysis of YgfO Helix XII

- Mol. Membr. Biol.* **22**, 263–275
- Karatza, P., Panos, P., Georgopoulou, E., and Frillingos, S. (2006) *J. Biol. Chem.* **281**, 39881–39890
  - Inoue, H., Nojima, H., and Okayama, H. (1990) *Gene (Amst.)* **96**, 23–28
  - Teather, R. M., Bramhill, J., Riede, I., Wright, J. K., Furst, M., Aichele, G., Wilhelm, V., and Overath, P. (1980) *Eur. J. Biochem.* **108**, 223–231
  - Ho, S. N., Hunt, H. D., Horton, R. M., Pullen, J. K., and Pease, L. R. (1989) *Gene (Amst.)* **77**, 51–59
  - Frillingos, S., Sahin-Tóth, M., Persson, B., and Kaback, H. R. (1994) *Biochemistry* **33**, 8074–8081
  - Carrasco, N., Herzlinger, D., Mitchell, R., DeChiara, S., Danho, W., Gabriel, T. F., and Kaback, H. R. (1984) *Proc. Natl. Acad. Sci. U. S. A.* **81**, 4672–4676
  - Granseth, E., Daley, D. O., Rapp, M., Melen, K., and von Heijne, G. (2005) *J. Mol. Biol.* **352**, 489–494
  - Frillingos, S., Sahin-Tóth, M., Wu, J., and Kaback, H. R. (1998) *FASEB J.* **12**, 1281–1299
  - Abramson, J., Smirnova, I., Kasho, V., Verner, G., Kaback, H. R., and Iwata, S. (2003) *Science* **301**, 610–615
  - Guan, L., Mizra, O., Verner, G., Iwata, S., and Kaback, H. R. (2007) *Proc. Natl. Acad. Sci. U. S. A.* **104**, 15294–15298
  - Pantazopoulou, A., and Diallinas, G. (2007) *FEMS Microbiol. Rev.* **31**, 657–675
  - Goudela, S., Reichard, U., Amillis, S., and Diallinas, G. (2008) *Fungal Genet. Biol.* **45**, 459–472
  - Argyrou, E., Sophianopoulou, V., Schultes, N., and Diallinas, G. (2001) *Plant Cell* **13**, 953–964